Indium Phosphide as a candidate sensor material for future large-scale thin film detectors

Device characterization and radiation hardness

Jennifer Ott, E.R. Almazan, T. McCoy, V. Fadeyev, A. Affolder, M. Hance, J. Nielsen, S. Kim, M. Jadhav, J. Metcalfe, A. Sumant

jeott@ucsc.edu
ottjenni@hawaii.edu

November 21, 2024
CPAD workshop

Thin-film detectors

Motivation and potential:

- Low mass, low material budget
- Large-scale manufacturing
- '3D integration' or monolithic detector: avoid hybridization for small pixels, keep low interconnect capacitance
- Different semiconductor materials

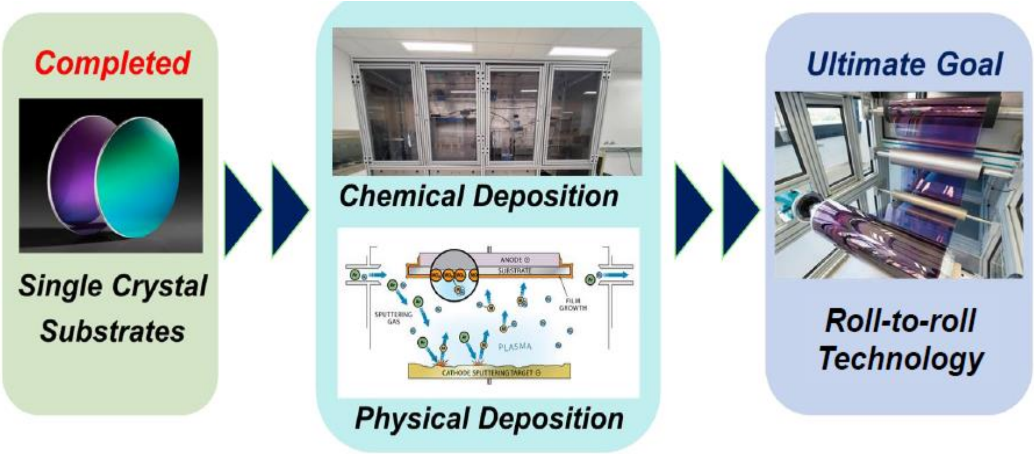

Thin-film growth methods are already used in detectors!

- High-resistivity epitaxial Si on low-res substrate, e.g. for LGADs: deposition is done as a thin film onto a substrate (of identical material and crystal structure), but result is a 'thick' substrate for hybrid detector
- CVD diamond: used for 'bulk' material deposition
- SiC: epitaxial growth of doped layers on crystalline bulk substrate
- Thick Si detectors which are ground down (ALICE ITS3) are not thin films in this sense…

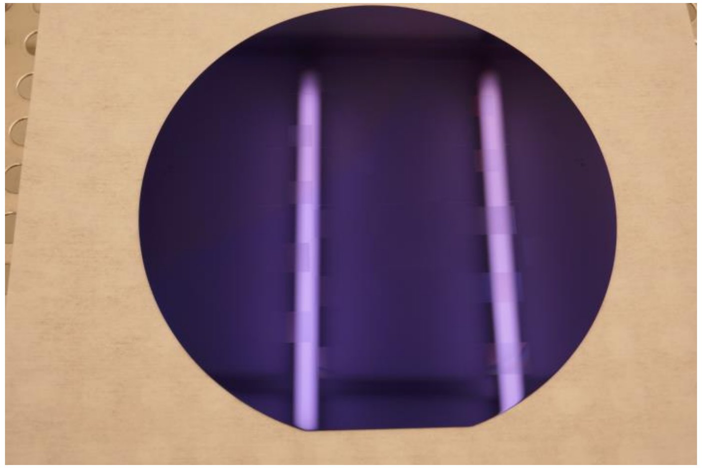

Examples on the path towards thin film particle tracking detectors shown here: crystalline material (InP) as test case and reference for thin film sensors

S. Kim et al, CPAD 2023

E. Almazan et al, CPAD 2023

Deposition methods & availability

Physical

- (Spin coating, dip coating)
- Sputtering
- Thermal evaporation
- E-beam evaporation
- Molecular beam epitaxy
- Ion- / laser beam assisted deposition

Chemical

- (Oxidation)
- Plating
- CVD
    - Plasma-enhanced CVD
- (MO)Vapour-phase epitaxy
- Atomic layer deposition

Facilities

- Individual labs or groups – often in Chemistry or Engineering departments
- Micro- / nanofabrication facilities at universities or national labs: e.g. Stanford, SLAC, ANL, BNL, LBNL
- Research institutes or semi-commercial centers, e.g. FBK, CNM, Sintef
- Commercial vendors

Thin film materials as charged particle detectors?

Sensor prototypes in InP: favorable properties, especially larger band gap and very high electron mobility

Chosen as a commercially available small wafer material and crystalline reference to (amorphous) future thin film devices

TABLE I

PROPERTIES OF SEMICONDUCTOR MATERIALS AT 25°C

Material	Atomic Number	Density g/cm³	Band-gap eV	Melting Point °C	Knoop Hardness	Crystal Structure	Ionicity	Dielectric Constant
Ge	32	5.33	0.67	958	692	Cubic	0	16
Si	14	2.33	1.12	1412	1150	Cubic	0	11.7
CdTe	48, 52	6.2	1.44	1092	45	Hexagonal	0.61	11
CdZnTe	48, 30, 52	≈ 6	1.5–2.2	1092–1295				
CdSe	48, 34	5.81	1.73	>1350		Hexagonal	0.6	10.6
CdZnSe	48, 30, 34	≈ 5.5	1.7–2.7	1239–1520				
HgI_2	80, 53	6.4	2.13	250 (127†)	<10	Tetragonal	0.67	8.8
TlBrI	81, 35, 53	7.5	2.2–2.8	405–480	40	Cubic		
GaAs	31, 33	5.32	1.43	1238	750	Cubic	0.23	12.8
InI	49, 53	5.31	2.01	351	27	Orthorhombic	0.8	26
GaSe	31, 34	4.55	2.03	960		Hexagonal	0.53	8
diamond	6	3.51	5.4	4027	10^4	Cubic	0	5.5
TlBr	81, 35	7.56	2.68	480	12	Cubic	0.81	29.8
PbI_2	82, 53	6.2	2.32	402	<10	Hexagonal	0.8	
InP	49, 15	4.78	1.35	1057	535	Cubic	0.38	12.5
ZnTe	30, 52	5.72	2.26	1295		Cubic	0.62	9.7
HgBrI	80, 35, 53	6.2	2.4–3.4	229–259	14	Orthorhombic		
a-Si	14	2.3	1.8				0	11.7
a-Se	34	4.3	2.3				0	6.6
BP	5, 15	2.9	2	d1400	4700	Cubic	0.01	11
GaP	31, 15	4.13	2.24	1750		Cubic		
CdS	48, 16	4.82	2.5	1477		Hexagonal	0.58	11.6
SiC	14, 6	3.2	2.2			Cubic		
AlSb	13, 51	4.26	1.62			Cubic		
PbO	82, 8	9.8	1.9	886				
BiI_3	83, 53	5.78	1.73	408		Hexagonal		
ZnSe	30, 34	5.42	2.58			Cubic		8.1

Note: Materials are listed in order of decreasing $\mu\tau(e)$ at room temperature.
*Estimated for 20% Zn.
**Estimated.
†Solid/solid phase transition.

TABLE I (*Continued*)

Material	E_{pair} eV	Resistivity (25°C) Ω-cm	Electron Mobility cm²/V · sec	Electron Lifetime sec.	Hole Mobility cm²/V · sec	Hole Lifetime sec.	$\mu\tau(e)$ Product cm²/V	$\mu\tau(h)$ Product cm²/V
Ge	2.96	50	3900	$>10^{-3}$	1900	1×10^{-3}	>1	>1
Si	3.62	up to 10^4	1400	$>10^{-3}$	480	2×10^{-3}	>1	≈1
CdTe	4.43	10^9	1100	3×10^{-6}	100	2×10^{-6}	3.3×10^{-3}	2×10^{-4}
CdZnTe	5.0*	10^{11}	1350	10^{-6}	120	5×10^{-8}	1×10^{-3}	6×10^{-6}
CdSe	5.5**	10^8	720	10^{-6}	75	10^{-6}	7.2×10^{-4}	7.5×10^{-5}
CdZnSe							$\approx 10^{-4}$	
HgI_2	4.2	10^{13}	100	10^{-6}	4	10^{-5}	10^{-4}	4×10^{-5}
TlBrI		10^{10}					9×10^{-5}	
GaAs	4.2	10^7	8000	10^{-8}	400	10^{-7}	8×10^{-5}	4×10^{-6}
InI		10^{11}					7×10^{-5}	
GaSe	4.5		75	5×10^{-7}	45	2×10^{-7}	3.5×10^{-5}	9×10^{-5}
diamond	13.25		2000	10^{-8}	1600	$<10^{-8}$	2×10^{-5}	$<1.6 \times 10^{-5}$
TlBr	6.5	10^{12}	6	2.5×10^{-6}			1.6×10^{-5}	1.5×10^{-6}
PbI_2	4.9	10^{12}	8	10^{-6}	2		8×10^{-6}	
InP	4.2	10^7	$\boxed{4600}$	1.5×10^{-9}	150	$<10^{-7}$	4.8×10^{-6}	$<1.5 \times 10^{-5}$
ZnTe	7.0**	10^{10}	340	4×10^{-9}	100	7×10^{-7}	1.4×10^{-6}	7×10^{-5}
HgBrI		5×10^{13}					1×10^{-6}	$<1 \times 10^{-7}$
a-Si	4	10^{12}	1	6.8×10^{-9}	.005	4×10^{-6}	6.8×10^{-8}	2×10^{-8}
a-Se	7	10^{12}	.005	10^{-6}	.14	10^{-6}	5×10^{-9}	1.4×10^{-7}
BP	6.5**	1	10	10^{-9}				
GaP	7.0**		120		120			
CdS	7.8**		300		50			
SiC	9.0**		400(α)					
AlSb	5.05	$<10^4$	300		400			
PbO	6.47							
BiI_3	5.5**	10^{12}						
ZnSe	8.0**		100					

Semiconductors for Room Temperature Nuclear Detector Applications

SEMICONDUCTORS AND SEMIMETALS Volume 43

InP sensor fabrication

Second batch: after first original device fabrication and test in proton beam

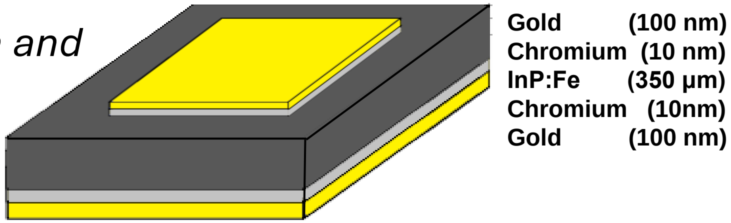

Single- and multipad devices fabricated by S. Kim at Argonne National Lab on commercial 2” InP:Fe wafers of 350 µm thickness

Both sides 10 nm / 100 nm Cr / Au

- Front side electrode design by e-beam evaporation and lift-off of patterned photoresist
- Backside sheet metallization by sputter deposition

➢**Single pad devices: 2x2 mm, one guard ring (100 µm) – half of the devices with a 150 µm optical opening**

➢**Multi-pad arrays: 25 pads, each 200x200 µm, 50 µm gap**

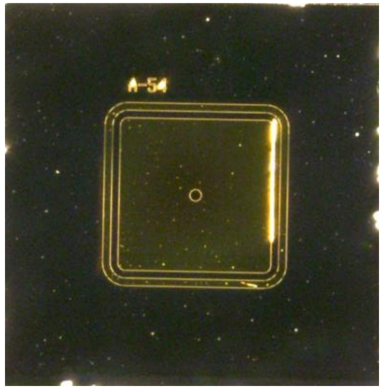

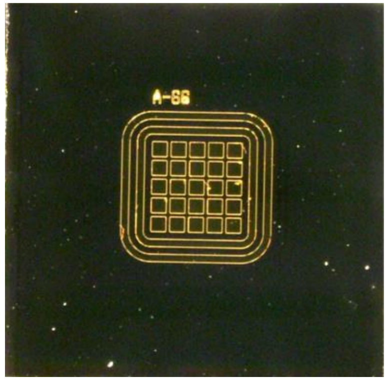

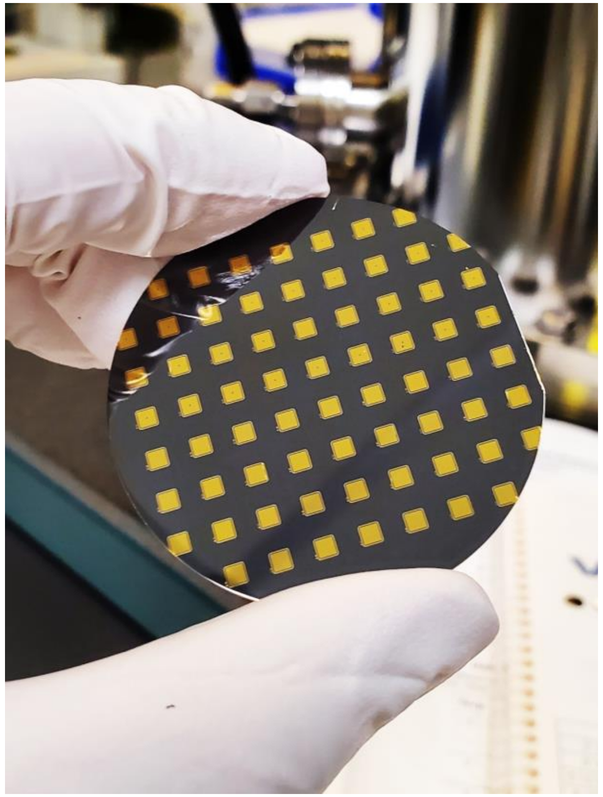

Capacitance for 2x2 mm pad: ca. 2 pF

Leakage currents higher than in Si, on the µA/mm² scale

- Relatively symmetrical in polarity
- Initially almost Ohmic behavior, then soft increase after 400 V
- No exponential breakdown before 600 V

Some samples exhibit rising capacitance and higher initial leakage current: apparently concentrated around a specific area on the wafer, close to a cut line

Crystalline InP sensors: X-ray test beams

Special thanks to L. Poley & test beam team!

- **Response of InP sensors to x-rays was studied at x-ray beam lines:**
  - Canadian Light Source (CLS)
  - Diamond Light Source (DLS)
- **Focused x-ray beams were scanned across the DUT – DC photocurrent response was measured at regular DUT stage position intervals; background subtracted**
  - No transient/pulse readout
- **Unexpected "persistent current" phenomenon: photocurrent persists for minutes after initial exposure to high-flux x-rays**
- **X-ray energy (15 keV) insufficient for complete device assessment - higher energy is needed to probe the full InP bulk uniformity**

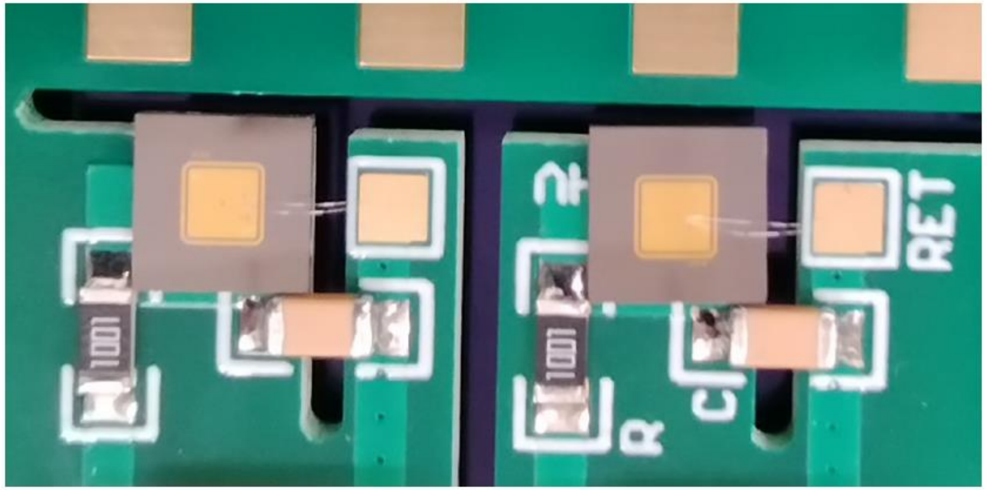

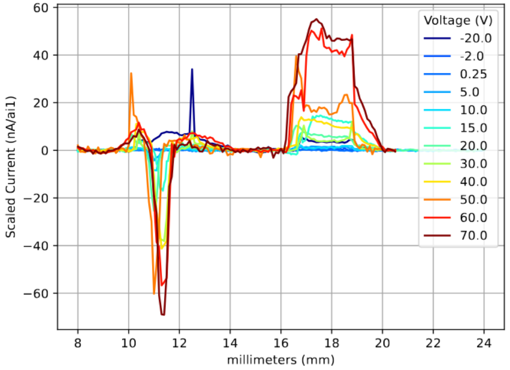

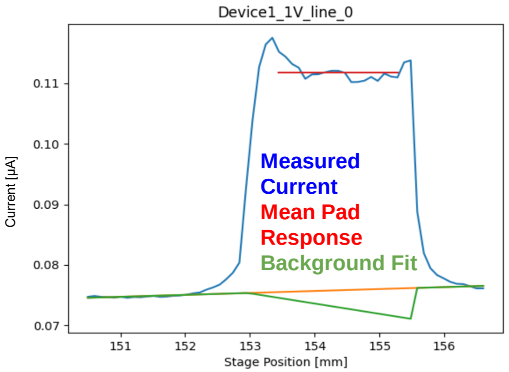

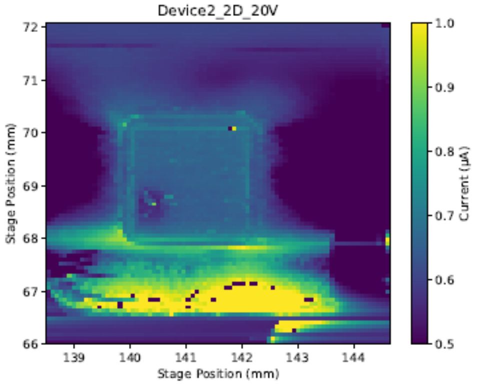

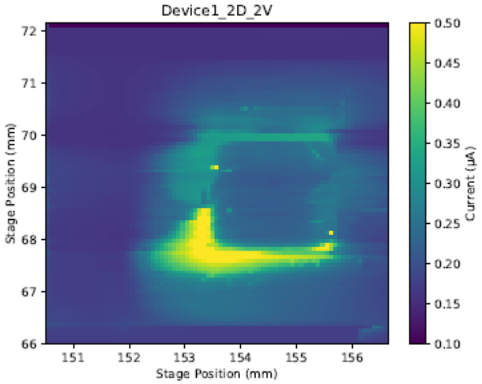

Crystalline InP sensors: beta source

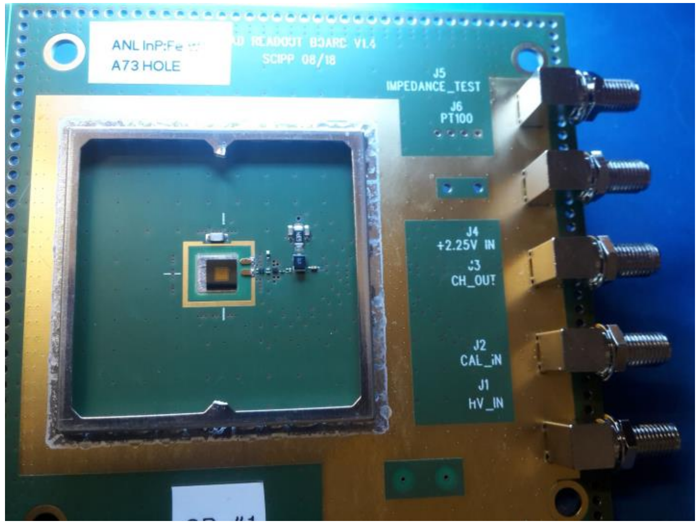

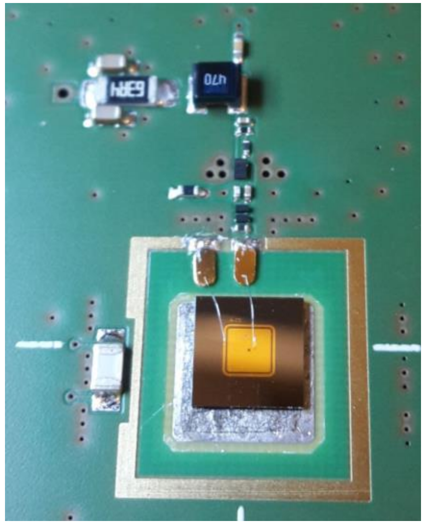

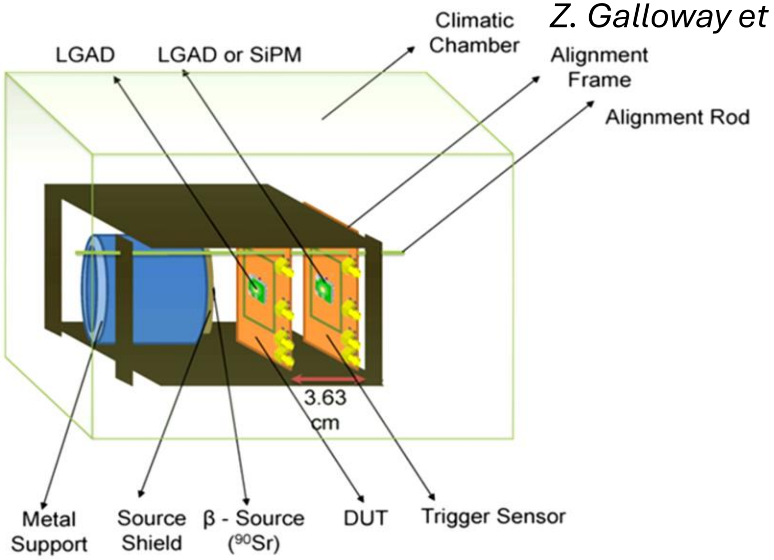

Z. Galloway et al 2019

350 µm single-pad sensor bonded to 1-ch UCSC fast readout board with 470 Ω transimpedance amplifier, second stage external 20dB RF amplifier

- Beta source: Sr-90
- Known HPK Silicon LGAD as trigger and timing reference

J. Ott, oral presentation, *Characterization of InP sensors for future thin film detectors*, 42nd RD50 Workshop

Manuscript in preparation

Crystalline InP sensors: beta source

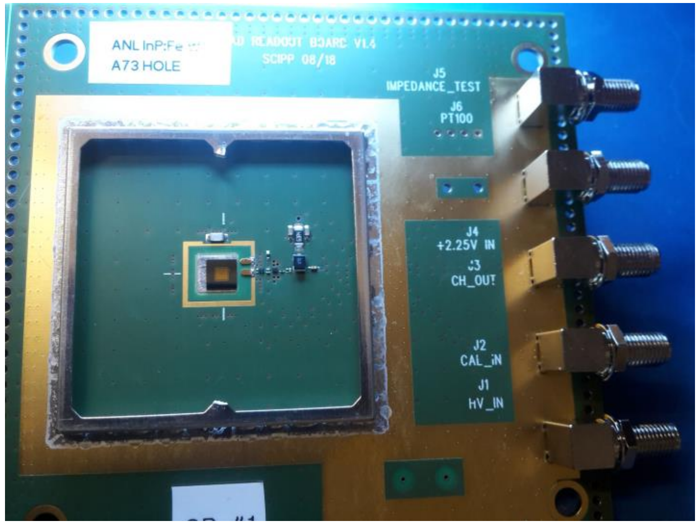

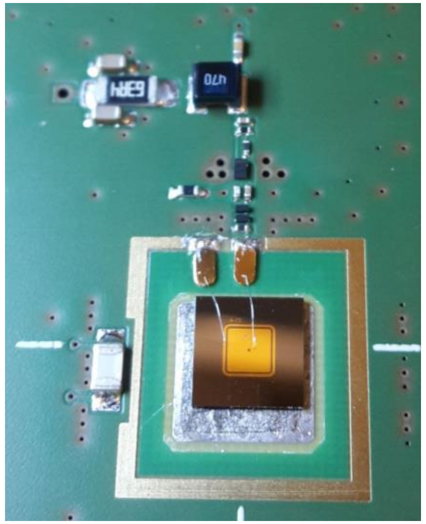

-20 C

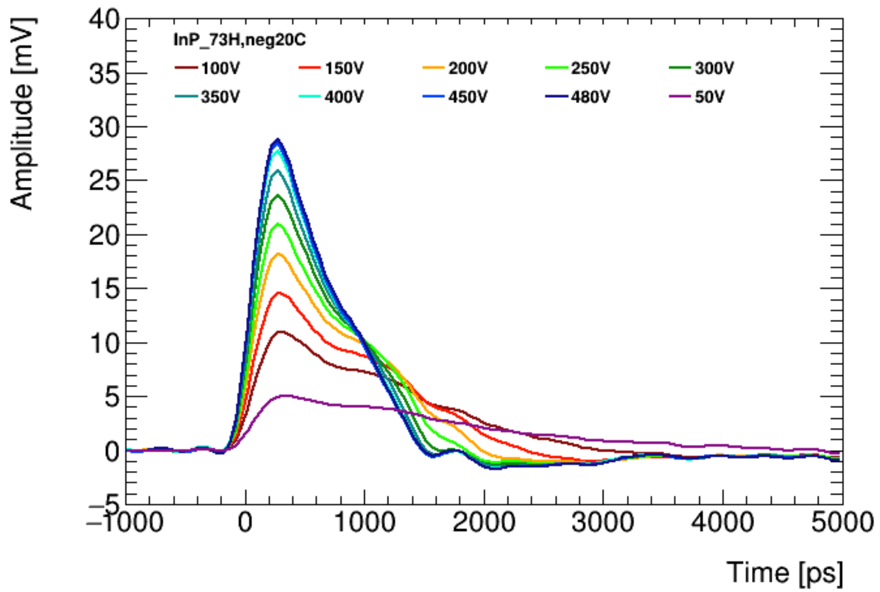

Performance:

- Comparatively small signal, around 15 mV at RT, but fast!
- Observed rise time independent of bias voltage, down to 250 ps after 150 V
- Excellent timing resolution: 33 ps reached between 300 and 400 V

- Sensor performance benefits from cooling: lower leakage, higher signal – typical for semiconductors, also Si
- Cooling from room temperature to 0 C has higher impact than cooling further down to -20 C

Temperature dependence of InP signal characteristics

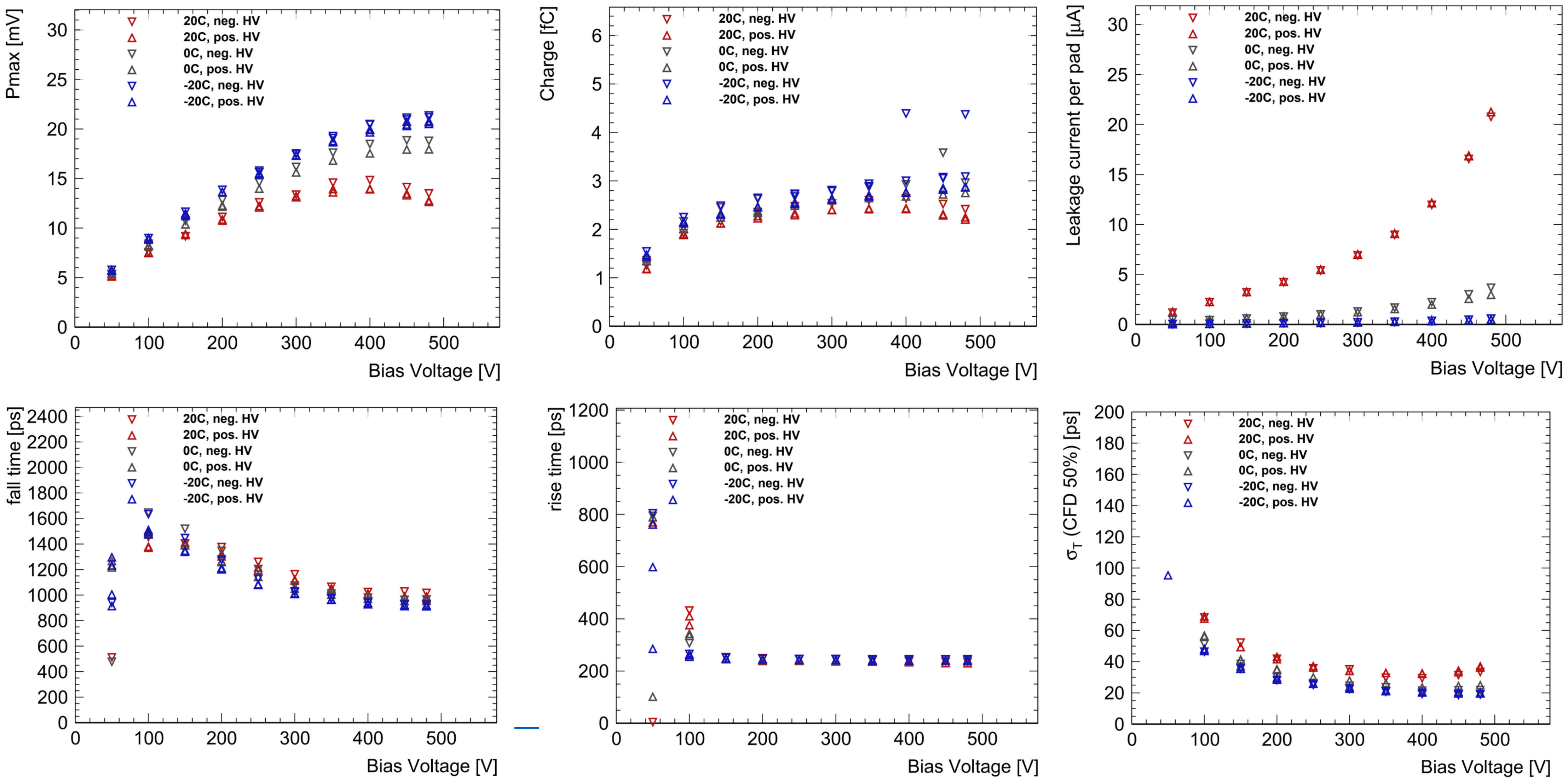

Irradiation of InP sensors

- **No established parameter space for radiation damage in InP as for silicon**
- **First irradiation study with single-pad sensors with a very wide fluence range: 1e13, 1e14, 1e15, 1e16 n/cm^2 at JSI/Ljubljana with 1 MeV neutrons (G. Kramberger)**

- **Comparatively high activation through neutron capture of ^{113}In (4.3% abundance) by ^{113}In (n, γ)^{114m1}In**
  - ^{114m1}In has a primary gamma emission at 190 keV, **$t_{1/2}$ ~50 days**
  - ^{114}In itself is short-lived (72 s), decays primarily to stable ^{114}Sn

- **To date (Nov 2024) fluences 1e13, 1e14, 1e15 n/cm^2 delivered back, 1e16 n/cm^2 not released yet**
  - 1e13, 1e14 n/cm^2 characterized, compared to pre-rad state (CV, IV) and unirradiated reference (Sr-90)
  - 1e15 n/cm^2 immediately reaching very high current at 1-5V
    - *Possible mechanical damage on at least one sample*
    - *Currently no cooling available for probe station: could attempt at mounting an irradiated sensor onto a single-channel board and test in cold in the betascope*

Irradiated InP sensors

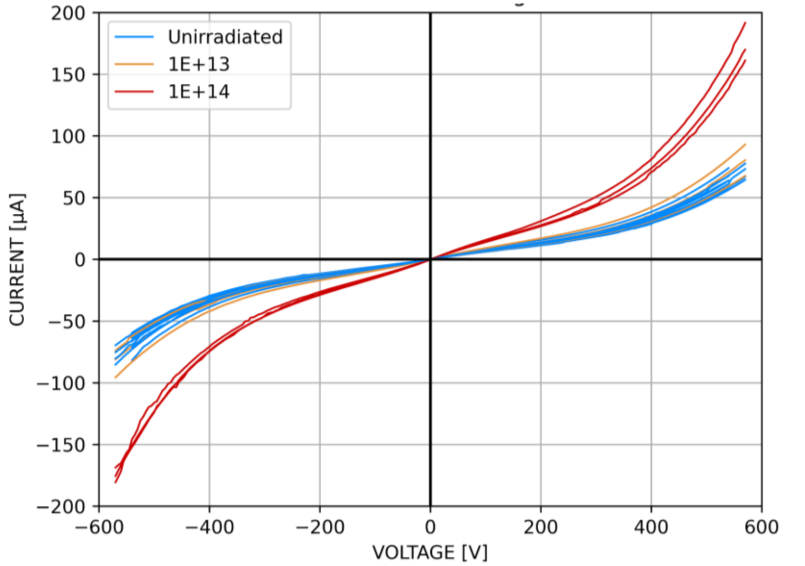

I-V and C-V:

- Higher leakage current, no change in capacitance

Betascope: same study, including temperature variation, for 1e13 and 1e14 samples

- Collected charge, pmax decrease – very low S/N ratio at 1e14
- Timing resolution is still very good at sufficient bias voltage and/or when cooled
- Rise time is faster in irradiated samples – approaches bandwidth limit of the preamplifier
- **350 μm bulk: future device design will have to select appropriate thickness for sufficient original signal charge, and efficient charge transport & low trapping in the bulk**

Waveforms at 300 V, higher bias voltages could not always be reached dure to leakage current

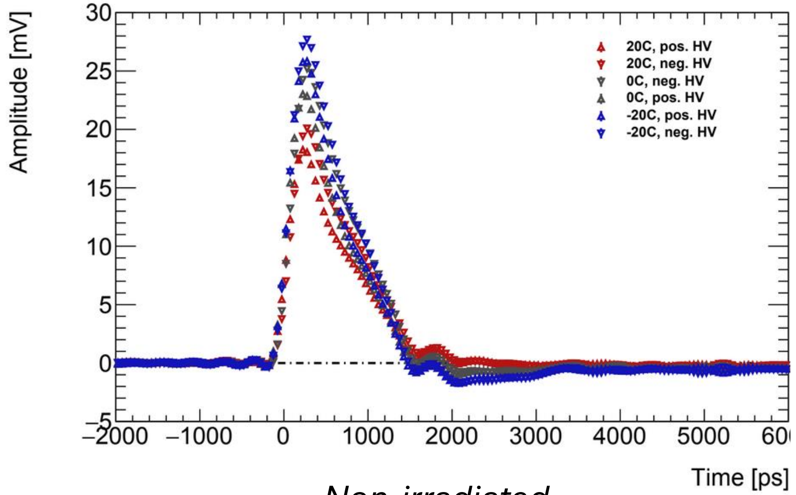

Non-irradiated

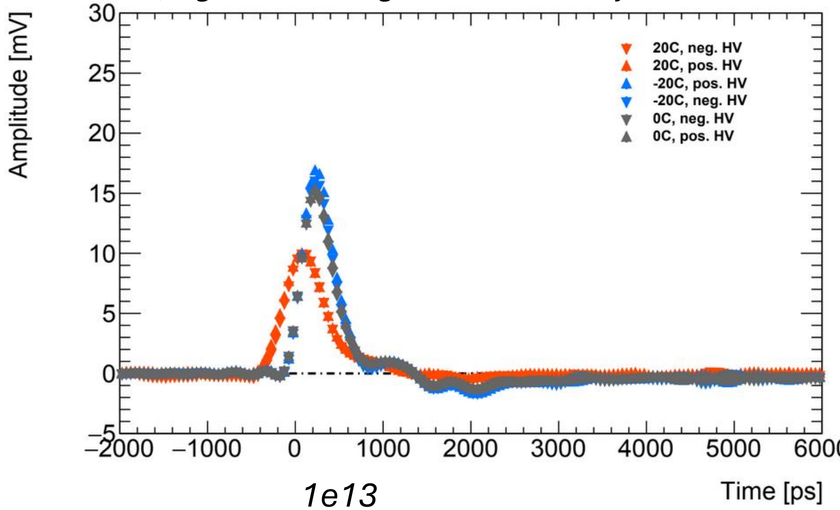

1e13

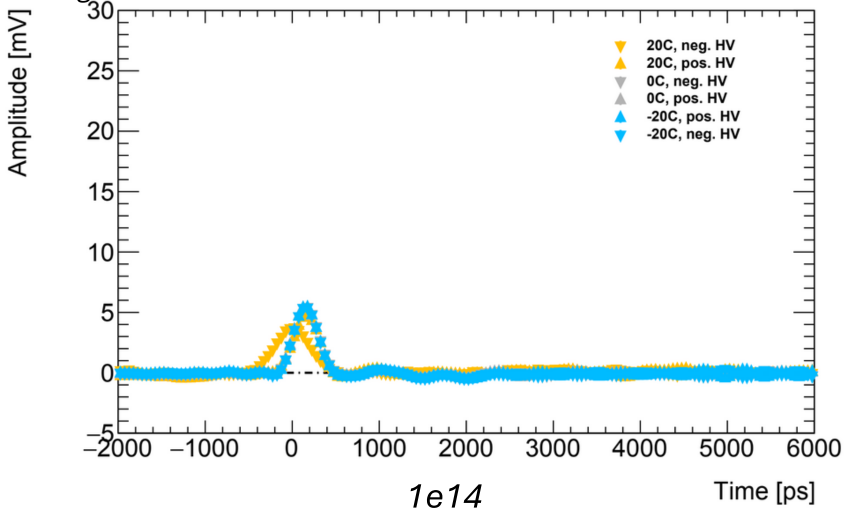

1e14

1e13

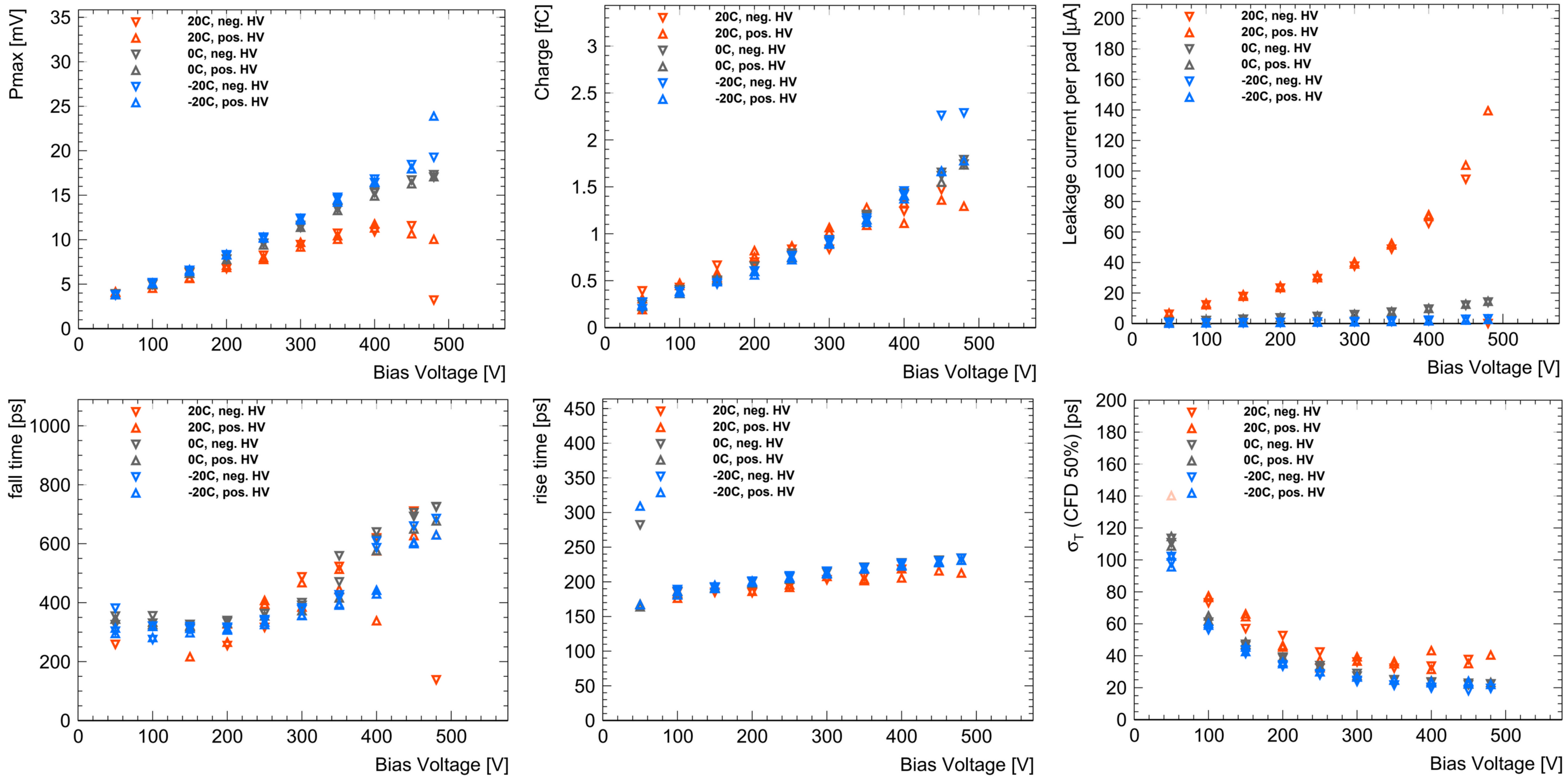
Pmax [mV]
Charge [fC]
Leakage current per pad [µA]
fall time [ps]
rise time [ps]
σ_T (CFD 50%) [ps]
Bias Voltage [V]
20C, neg. HV
20C, pos. HV
0C, neg. HV
0C, pos. HV
-20C, neg. HV
-20C, pos. HV

1e14

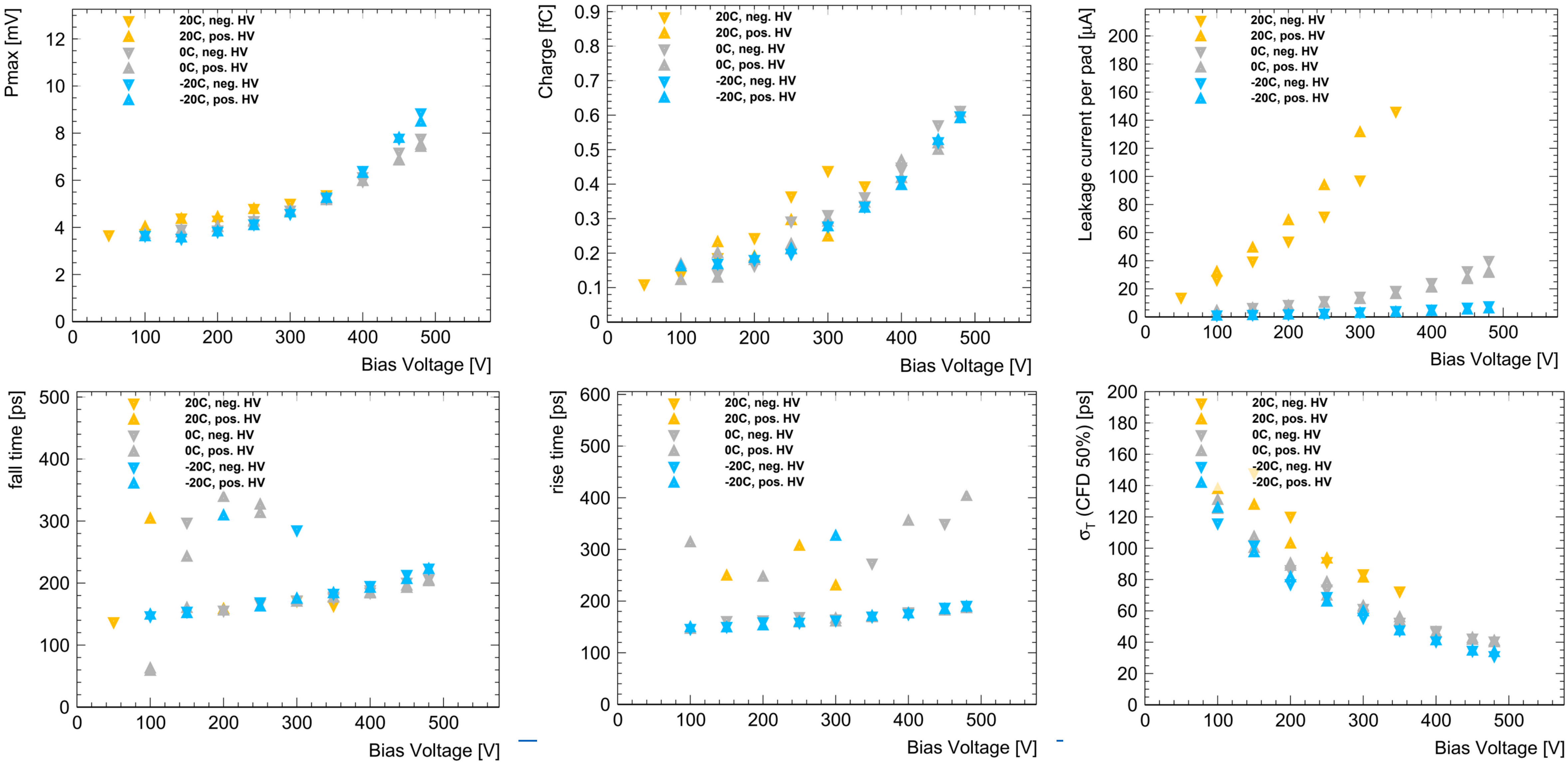
Pmax [mV]
Bias Voltage [V]
Charge [fC]
Leakage current per pad [µA]
fall time [ps]
rise time [ps]
σ_T (CFD 50%) [ps]
20C, neg. HV
20C, pos. HV
0C, neg. HV
0C, pos. HV
-20C, neg. HV
-20C, pos. HV

Irradiated InP sensors

Comparison at -20 C / best performance

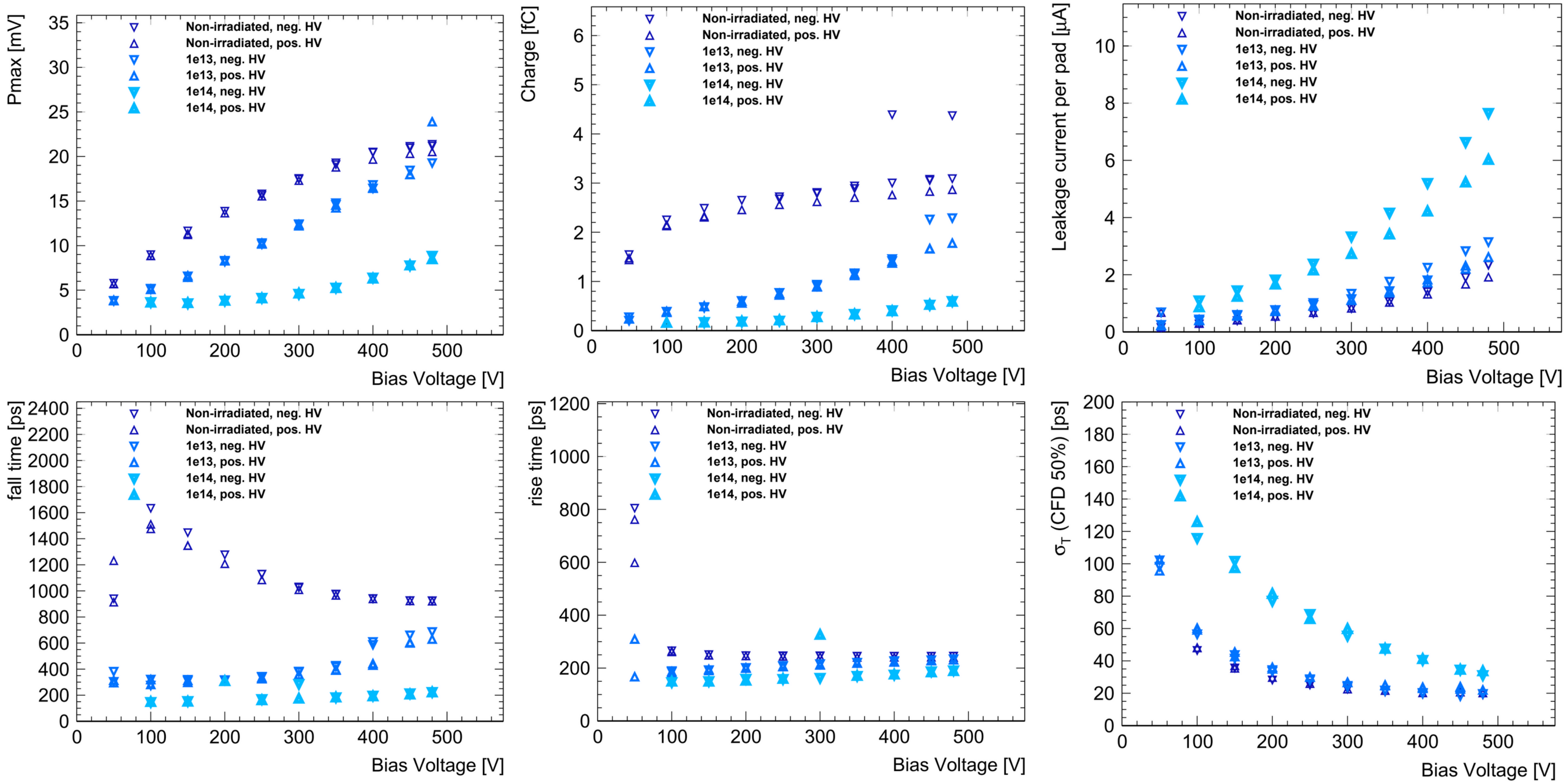

Conclusions; status and next steps

- **Towards depositing InP (and/or other materials of interest) as amorphous thin films: CVD machine at ANL purchased and installed – to be commissioned**
  - Selection and ordering of precursor chemicals: involvement of chemical and laboratory safety officers

- **(Re)Commissioning of AliBava setup with mother- and daughter board for triggering and DAQ**
- **Thorlabs thermal camera imaging setup for identifying possible current hotspots in InP (and Si) sensors**

- **Further x-ray test beams at DLS and CLS**
- **Charged particle test beam?**

- **Continue testing of multi-pad sensors**
- **Irradiation of sensors with charged particles; ionizing dose**

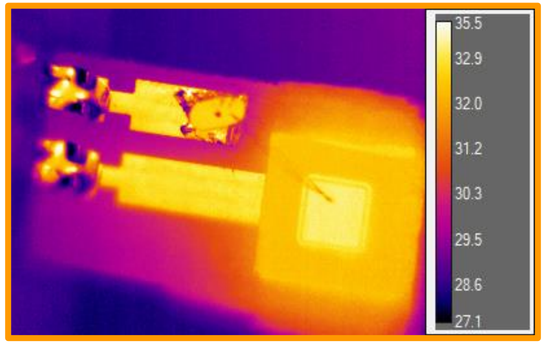

References

S. Kim, V. Berry, J. Metcalfe, A.V. Sumant, *Thin film charged particle detectors*, JINST 18 (2023)

S. Kim, M. Jadhav, V. Berry, J. Metcalfe, A.V. Sumant, *Novel indium phosphide charged particle detector characterization with a 120 GeV proton beam*, JINST 19 (2024) P08016

E.R. Almazan, A. Affolder, V. Fadeyev, M. Hance, M. Jadhav, S. Kim, T. McCoy, J. Metcalfe, J. Nielsen, J. Ott, L. Poley, T.(K.-W.) Shin, D. Sperlich, A. Sumant, *Characterizing novel Indium Phosphide pad detectors with focused X-ray beams and laboratory tests*, JINST 19 (2024) P11016

J. Ott et al, *Characterization of temporal response and irradiation studies of InP sensors* – in preparation

Bonus

Amorphous Selenium; deposition on ASIC (ITkPix)

aSe is most established as x-ray detector for e.g. mammography panels

Approach here: utilize pixelated ASIC developed for HEP, deposit active sensor material directly on top by relatively low-temperature thermal evaporation

- Using ITkpixV1.0 (RD53B), V2.0 (recent)
- Leveraging expertise with ATLAS pixel modules to set up DAQ, perform chip calibrations and tuning before scans with radioactive source

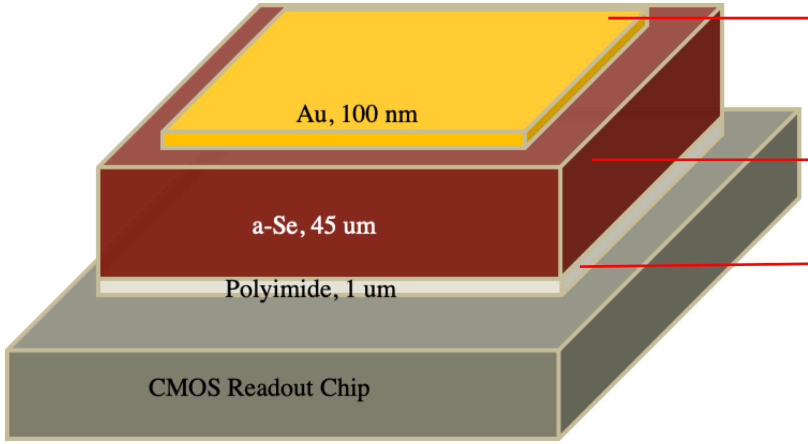

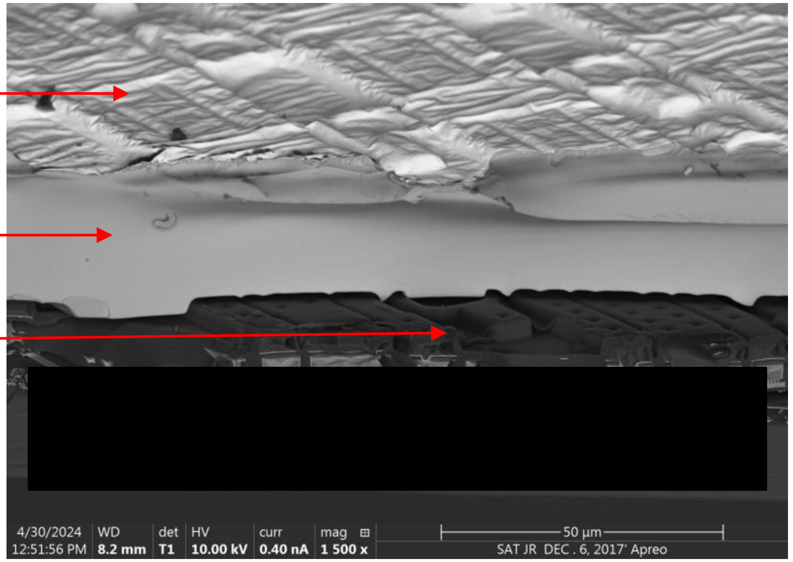

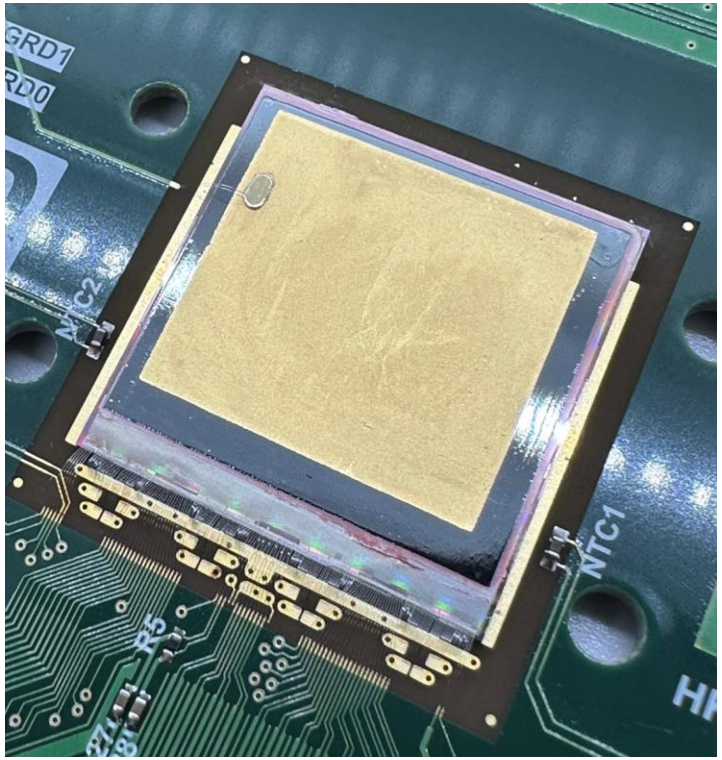

A. Swaby, **J. Ott**, K. Hellier, M. Garcia-Sciveres, S. Abbaszadeh, *Hybrid a-Se/RD53B CMOS Detector: Initial Results*, Proceedings of SPIE Medical Imaging (2023), 12463, https://doi.org/10.1117/12.2654519

Amorphous Selenium; deposition on ASIC (ITkPix)

First prototype of ITkPix v2 chip with aSe film tested this summer

Regular testing routine (communication/eye diagram), digital & analog scan, tuning of threshold

- Deactivation of some edge columns was needed

Source scans with Kr-85 low-energy beta source and tabletop x-ray gun: effect of sensor bias voltage on hit rate and ToT well visible

Next steps: evaluation of aSe thickness, further tuning of preamplifier feedback → ToT response

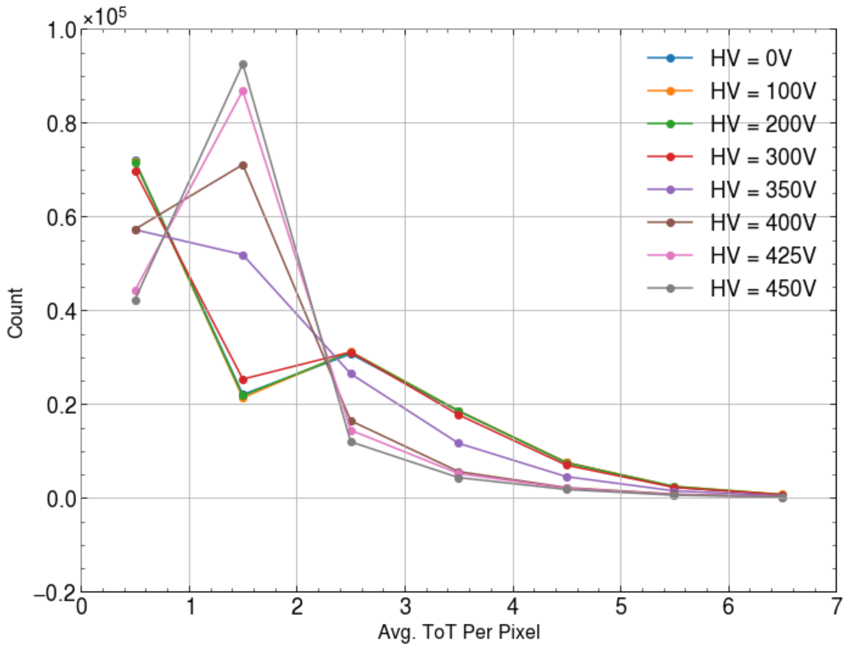

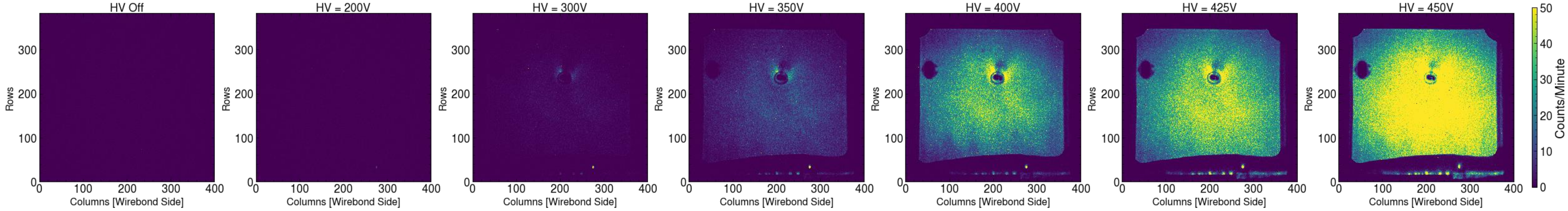

J. Ott, A. Swaby, K. Hellier, L. Le Pottier, M. Mironova, T. Heim, C. Hultquist, M. Garcia-Sciveres, S. Abbaszadeh, *a-Se thin film detector on ITkpix CMOS readout: time-over-threshold tuning and pixel performance analysis*, SPIE Medical Imaging February 2025

Thank you!

Backup

Materials of interest for charged particle tracking?

- (Si)
- InP
- CdTe, CZT?
- GaAs?
- InGaAs?
- Thin diamond?
- SiC?
- *Others?*

TABLE I

PROPERTIES OF SEMICONDUCTOR MATERIALS AT 25°C

TABLE I (*Continued*)

Material	Atomic Number	Density g/cm³	Band-gap eV	Melting Point °C	Knoop Hardness	Crystal Structure	Ionicity	Dielectric Constant	E_{pair} eV	Resistivity (25°C) Ω-cm	Electron Mobility cm²/V · sec	Electron Lifetime sec.	Hole Mobility cm²/V · sec	Hole Lifetime sec.	$\mu\tau(e)$ Product cm²/V	$\mu\tau(h)$ Product cm²/V
Ge	32	5.33	0.67	958	692	Cubic	0	16	2.96	50	3900	$>10^{-3}$	1900	1×10^{-3}	>1	>1
Si	14	2.33	1.12	1412	1150	Cubic	0	11.7	3.62	up to 10^4	1400	$>10^{-3}$	480	2×10^{-3}	>1	≈1
CdTe	48, 52	6.2	1.44	1092	45	Hexagonal	0.61	11	4.43	10^9	1100	3×10^{-6}	100	2×10^{-6}	3.3×10^{-3}	2×10^{-4}
CdZnTe	48, 30, 52	≈ 6	1.5–2.2	1092–1295					5.0*	10^{11}	1350	10^{-6}	120	5×10^{-8}	1×10^{-3}	6×10^{-6}
CdSe	48, 34	5.81	1.73	>1350		Hexagonal	0.6	10.6	5.5**	10^8	720	10^{-6}	75	10^{-6}	7.2×10^{-4}	7.5×10^{-5}
CdZnSe	48, 30, 34	≈ 5.5	1.7–2.7	1239–1520											$\approx 10^{-4}$	
HgI_2	80, 53	6.4	2.13	250 (127†)	<10	Tetragonal	0.67	8.8	4.2	10^{13}	100	10^{-6}	4	10^{-5}	10^{-4}	4×10^{-5}
TlBrI	81, 35, 53	7.5	2.2–2.8	405–480	40	Cubic				10^{10}					9×10^{-5}	
GaAs	31, 33	5.32	1.43	1238	750	Cubic	0.23	12.8	4.2	10^7	8000	10^{-8}	400	10^{-7}	8×10^{-5}	4×10^{-6}
InI	49, 53	5.31	2.01	351	27	Orthorhombic	0.8	26		10^{11}					7×10^{-5}	
GaSe	31, 34	4.55	2.03	960		Hexagonal	0.53	8	4.5		75	5×10^{-7}	45	2×10^{-7}	3.5×10^{-5}	9×10^{-5}
diamond	6	3.51	5.4	4027	10^4	Cubic	0	5.5	13.25		2000	10^{-8}	1600	$<10^{-8}$	2×10^{-5}	$<1.6 \times 10^{-5}$
TlBr	81, 35	7.56	2.68	480	12	Cubic	0.81	29.8	6.5	10^{12}	6	2.5×10^{-6}			1.6×10^{-5}	1.5×10^{-6}
PbI_2	82, 53	6.2	2.32	402	<10	Hexagonal	0.8		4.9	10^{12}	8	10^{-6}	2		8×10^{-6}	
InP	49, 15	4.78	1.35	1057	535	Cubic	0.38	12.5	4.2	10^7	4600	1.5×10^{-9}	150	$<10^{-7}$	4.8×10^{-6}	$<1.5 \times 10^{-5}$
ZnTe	30, 52	5.72	2.26	1295		Cubic	0.62	9.7	7.0**	10^{10}	340	4×10^{-9}	100	7×10^{-7}	1.4×10^{-6}	7×10^{-5}
HgBrI	80, 35, 53	6.2	2.4–3.4	229–259	14	Orthorhombic				5×10^{13}					1×10^{-6}	$<1 \times 10^{-7}$
a-Si	14	2.3	1.8				0	11.7	4	10^{12}	1	6.8×10^{-9}	.005	4×10^{-6}	6.8×10^{-8}	2×10^{-8}
a-Se	34	4.3	2.3				0	6.6	7	10^{12}	.005	10^{-6}	.14	10^{-6}	5×10^{-9}	1.4×10^{-7}
BP	5, 15	2.9	2	dl400	4700	Cubic	0.01	11	6.5**	1	10	10^{-9}				
GaP	31, 15	4.13	2.24	1750		Cubic			7.0**		120		120			
CdS	48, 16	4.82	2.5	1477		Hexagonal	0.58	11.6	7.8**		300		50			
SiC	14, 6	3.2	2.2			Cubic			9.0**		400(α)					
AlSb	13, 51	4.26	1.62			Cubic			5.05	$<10^4$	300		400			
PbO	82, 8	9.8	1.9	886					6.47							
BiI_3	83, 53	5.78	1.73	408		Hexagonal			5.5**	10^{12}						
ZnSe	30, 34	5.42	2.58			Cubic		8.1	8.0**		100					

Note: Materials are listed in order of decreasing $\mu\tau(e)$ at room temperature.
*Estimated for 20% Zn.
**Estimated.
†Solid/solid phase transition.

Semiconductors for Room Temperature Nuclear Detector Applications

SEMICONDUCTORS AND SEMIMETALS
Volume 43

InP wafer specifications

QUALITY TEST REPORT

Date:SEP.03,2021
PO#:1A-75205
PI#:PW21219

Description:2" InP wafers
Customer:ARGONNE NATIONAL LABORATORY

Parameter	Customer's Requirements	Guaranteed / Actual Values	UOM
Material	InP	InP	
Conduct Type/Dopant	SI/Fe	SI/Fe	
Diameter:	50.8±0.2	50.8±0.2	mm
Orientation:	(100)±0.5°	(100)±0.5°	
Flat Option	EJ	EJ	
Primary Flat Orientation:	(0-1-1)	(0-1-1)	
Primary Flat Length:	16±1	16±1	mm
Secondary Flat Orientation:	(0-11)	(0-11)	
Secondary Flat Length:	7±1	7±1	mm
Resistivity:	Min：1E7 Max：/	Min：1.96E7 Max：/	cm^{-3}
Mobility:	Min：2000 Max：/	Min：2650 Max：/	
EPD:	Ave：<5000 Max：/	Ave：<2251 Max：/	cm^{-2}
Laser Marking	Back side major flat	Back side major flat	
Edge Rounding	0.25(Conform to SEMI Standards)	0.25(Conform to SEMI Standards)	mmR
Thickness:	Min：325 Max：375	Min：325 Max：375	um
TTV:	Max：10	Max：10	um
BOW:	Max：10	Max：10	um
Warp:	Max：15	Max：15	um
Suface:	Side 1:Polished Side 2:etched	Side 1:Polished Side 2:etched	
Package	individual container filled with N_2	individual container filled with N_2	
Epi-ready	Yes	Yes	
Quantity:	5	5	pcs

Wafer No.: X-35F1355B002 X-35F1265A020 X-35F1265A021 X-35F1265A022 X-35F1265A028

Prepared by:Ximing Zhang

Checked by:Wenyuan Liu(ID0401)
SEP.03,2021

Approved by:Shipeng Wang
SEP.03,2021